

Chapter 7

Conclusions and Future Work

“I think it is much more interesting to live with uncertainty than to live with answers that might be wrong”

by Richard Feynman

This chapter summarizes research outcomes of the thesis and highlights some relevant future scopes.

Contents

7.1	Summary of work done	216
7.1.1	Regional GPS network and surface velocity field	216
7.1.2	Geodetic strain rate field	216
7.1.3	Slip rate distribution of the Himalayan megathrust system	217
7.1.4	Spatial distribution of earthquake potential	217
7.1.5	Earthquake potential score of populous Himalayan cities	217
7.2	Major findings of the study	218
7.3	Contributions through this research	219
7.4	Future scope of the present research work	220

7.1 Summary of work done

One of the widely used techniques to monitor crustal movements is the repeated geodetic measurements. In this thesis, the main aim is to characterize interseismic crustal deformation and consequent earthquake potential evaluation along the Himalayan arc using a dense GPS network. Below, a chapter-wise summary of the work done is mentioned.

7.1.1 Regional GPS network and surface velocity field

After a theoretical overview of the Himalayan arc in Chapter 1 and an explicit literature review on seismic hazard studies in Chapter 2, the contemporary surface velocity field along the Himalayan arc was derived in Chapter 3 through a number of successive tasks, such as the setting up of a regional GPS network, data collection, data processing, and its analysis. First, GPS data were collected from a regional GPS network comprising three arc-normal (T1, T2, and T3) transects and one arc-parallel (T4) transect encompassing the Himalayan megathrust system. The accrued GPS data from this network were processed using the GAMIT-GLOBK suite of post-processing software and the GPS velocity vectors along with daily position time-series plots were derived.

The surface velocity field (ITRF08 frame) in all the four transects showed a general northeast directed motion. It was observed that the surface velocities (ITRF08 frame) gradually increase from west to east direction. In order to increase the spatial resolution of the surface velocity field along the Himalayan arc, an updated set of 446 published horizontal velocities were combined in a common reference frame.

7.1.2 Geodetic strain rate field

The derived surface velocity field in Chapter 3 was utilized to calculate the geodetic strain rate field in terms of dilatation, maximum shear, and rotation strain rates. The dilatation strain rates represent extension and compression in the region, whereas the maximum shear strain describes strike-slip motion. It was observed that the compressional strain rates were dominant because of the India-Eurasia tectonic collision, though there were some patches of extensional strain rates along the Hindu-Kush, Pamir, and the Tibetan Plateau. Higher maximum shear strain rates were inferred along the MCT region. The rotation rates reflected the general pattern of the surface velocity field along the Himalayan arc.

7.1.3 Slip rate distribution of the Himalayan megathrust system

In Chapter 4, to characterize the slip rate distribution of the megathrust system along the Himalayan arc, the surface velocity field was inverted from 15 arc-normal velocity profiles along the strike of the Himalayan arc using a two-dimensional Bayesian splay-fault model. In the Bayesian model, the apriori information of fault parameters (e.g., dip angle, rake angle, strike angle, fault surface location, locking depth, down-dip depth, etc.) were collected from the geological studies. To estimate the joint posterior distribution of fault parameters and fault slip, a Markov Chain Monte Carlo (MCMC) method was employed incorporating the Metropolis algorithm. The slip rate estimates of MFT and MBT suggested the progression of their locking behavior, starting from northwest Himalaya, continuing to the central Himalaya, and further extending up to the northeast Himalaya. The slip rates of the MCT and MHT were observed to be higher along the northwest and the central Himalaya, whereas it was observed to be lesser along the northeast Himalaya. These slip rates of the MFT, MBT, MCT, and the MHT provided the evidence of coupling from surface to down-dip end of the Himalayan megathrust system.

7.1.4 Spatial distribution of earthquake potential

To derive the spatial distribution of earthquake potential along the Himalayan arc, a segmentation-based approach was considered in Chapter 5. The study area was divided into 24 seismogenic zones based on the distinctly different seismo-tectonic characterization. Further, the geodetic strain rates were translated into geodetic moment rates and compared with seismic moment rates derived from ~ 900 years of seismicity data in each segment. The geodetic moment rates represent seismic energy accumulation, whereas the seismic moment rates indicate energy release. The comparison of these two provides a total energy budget that could possibly generate future devastating earthquakes. The segments with high seismic potential are observed to correspond to the postulated seismic gaps, whereas lower earthquake potential corresponds to the segments encompassing the rupture areas of recent large events.

7.1.5 Earthquake potential score of populous Himalayan cities

After the earthquake potential evaluation from geodetic methods, a statistical nowcasting approach was implemented in Chapter 6 to determine the current state of earthquake

hazard at dozens of populous cities along the Himalayan arc and its adjacent regions. In this method, the number of intermittent “small” magnitude events between the pairs of “large” earthquakes were counted and a number of probability distributions were utilized to estimate the Earthquake Potential Score (EPS) of a defined circular city region. The EPS scores, like “thermometer” readings, describe the “current” level of seismic progression of a city in its earthquake cycle of large events. The estimated EPS scores above 80% at several cities indicate that these cities have reached their rear end in the seismic cycle of large earthquakes.

Seismic hazard analyses using the geodetic methods (Chapter 3 to Chapter 5) and the statistical method (Chapter 6) are all related to the concept of the elastic rebound theory. While the geodetic approach has provided a long-term perspective of moment build-up, the proposed nowcasting approach has evaluated the current progression of the seismic cycle in several local city regions. A combination of these two methods has provided a snapshot of high seismic hazard areas along the Himalayan arc.

In summary, the present thesis work has better characterized the ongoing crustal deformation in terms of the updated surface velocity field, strain rate patterns, fault kinematics of the megathrust system, and the spatial distribution of earthquake potential along the Himalayan arc. The findings will provide invaluable inputs to the time-dependent seismic hazard analysis of the study region.

7.2 Major findings of the study

The major findings of the present study are highlighted below.

1. The horizontal velocities from 40 regional and 446 published data vary between 37 mm/yr and 56 mm/yr with uncertainties lying in the range of 2–3 mm/yr. Overall, the direction of the horizontal velocity field is oblique along the northwest Himalaya and the northeast Himalaya, and it is purely arc-normal along the central Himalaya.
2. The geodetic dilatation strain rates indicate that the compressional rates (–150 nstrain/yr to –200 nstrain/yr) are more dominant than the extensional rates (80 nstrain/yr to 90 nstrain/yr). The higher maximum shear strain rates are observed in the north of the MCT along the central and the northeast Himalaya.

3. The persistent locking behavior of both MFT and MBT is observed along the entire Himalayan region, whereas the higher slip rates of MCT (~ 4.2 mm/yr to ~ 13.8 mm/yr) and MHT ($\sim 13.8 \pm 3.1$ mm/yr) are observed along the Himalayan arc.
4. The estimated geodetic moment rate ranges from 1.7×10^{18} Nm/yr to 10.2×10^{18} Nm/yr, whereas the seismic moment rate ranges from 3.7×10^{16} Nm/yr to 5.1×10^{19} Nm/yr. This variation between the geodetic and seismic moment rate corresponds to a moment deficit rate of $\sim 1.15 \times 10^{17}$ Nm/yr to 7.97×10^{18} Nm/yr along various segments of the study region.
5. Based on the comparison between moment accumulation rate and moment release rate, an earthquake potential of magnitude 5.7 – 8.2 is observed along 24 segments of the Himalayan arc. Specifically, the higher earthquake potential ($M_w \geq 8.0$) corresponds to the segments in the central seismic gap and the northeast part of Himalaya, whereas the lower earthquake potential ($M_w < 7.0$) corresponds to the segments encompassing the rupture areas of recent large events.
6. Based on the nowcasting analysis, it is found that the EPS scores for most of the cities along the Himalayan arc lie in the range of 80% and 99%. The EPS for cities along the northwest Himalaya is alarmingly high, except New Delhi (56%) and Peshawar (38%); the EPS for cities along the central Himalaya suggests that almost all the cities, except Ghorahi (67%) and Tulsipur (59%), have reached to their rear end of earthquake cycle; the EPS for cities along the northeast Himalaya varies between 41% to 94%, with the scores (>75%) of Agartala (91), Darjeeling (81), Dhaka (78), Dimapur (80), Imphal (90), and Silchar (87).

7.3 Contributions through this research

The present research has the following contributions towards the understanding of Himalayan tectonics.

1. The present thesis work provides a comprehensive horizontal velocity field along the entire Himalayan arc.
2. It brings out the most updated geodetic strain field along the entire Himalayan arc in terms of the regions of compression, extension, and strike-slip motion.

3. The estimated slip rate distribution along the megathrust system characterizes the coupling zone and creeping zone along the Himalayan arc.
4. Comparison of geodetic moment rates and seismic moment rates provides the spatial distribution of the earthquake potential along the entire Himalayan arc, highlighting the segments of higher earthquake potential.
5. The proposed natural time analysis has provided a way to examine the current state of earthquake hazard at dozens of populous cities along the Himalayan arc. This enables a ranking of cities based on their current seismic exposure.
6. Finally, the surface velocity field, estimated strain rates, slip rate distribution, and contemporary earthquake potential contribute to the seismic hazard analysis of the Himalayan arc.

7.4 Future scope of the present research work

A number of future researches that can be developed and/or integrated as an advancement of the present thesis work are listed below.

1. **Modeling of the aseismic strain in the estimation of earthquake potential:** Aseismic activities over a fault, as opposed to the locking behavior of the fault, are often considered as less likely to generate large earthquakes due to the lack of long-term strain accumulation. Hence, modeling and quantifying the aseismic contribution in the total strain accumulation will provide a more realistic figure of the stored energy, contributing to the estimation of the current earthquake potential along the Himalayan arc.
2. **Uncertainty analysis:** Understanding the impact of variation in all parameters together (e.g., uncertainty in geodetic velocities, seismic/aseismic contribution in strain accumulation, uncertainty in seismogenic depth, choice of the smoothness parameter in strain rate computation, consideration of the length of earthquake catalog) through the principle of propagation of uncertainty can provide a better hazard estimation along with its possible confidence intervals. A possible tree diagram (Fig. 7.1) of uncertainty quantification and propagation in the earthquake potential is provided below.

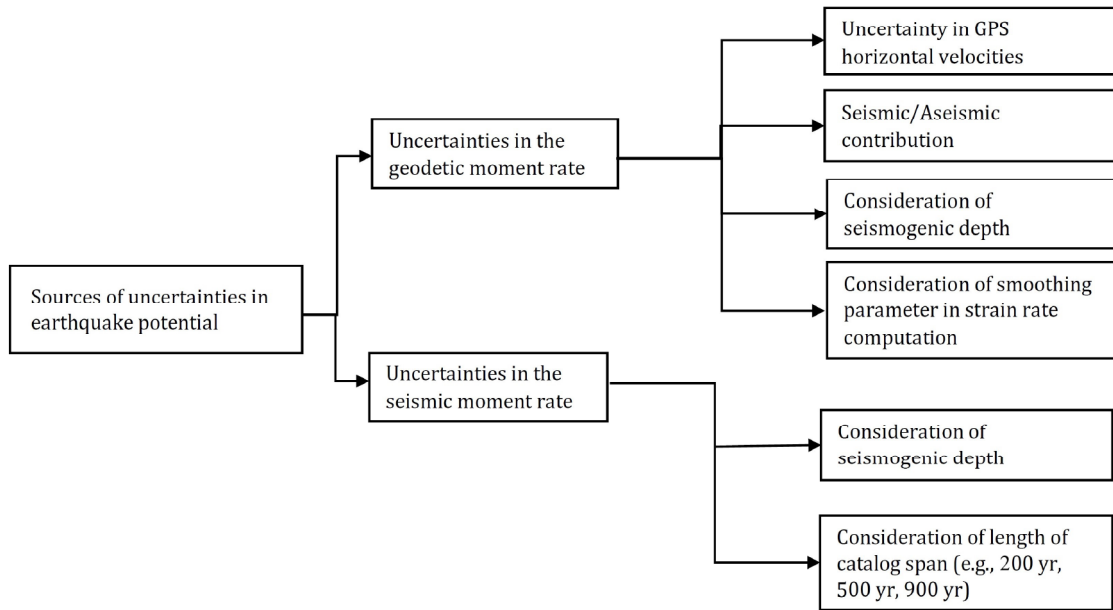


Fig. 7.1: Tree diagram of uncertainty quantification and propagation in the earthquake potential.

3. **Integration of GPS and InSAR data for the high-resolution crustal deformation:** The GPS observations are often used to measure the three-dimensional deformation signals at discrete locations, whereas the InSAR observations are used to measure the areal deformation signals in the line-of-sight direction of the satellite. Therefore, these techniques are complementary to each other and integrating these two observation methods will provide more insights to the spatio-temporal resolution of the crustal deformation pattern.
4. **Development of a three-dimensional inversion model for the crustal deformation:** A general three-dimensional dislocation model not only provides the surface deformation but also enables us to estimate the vertical deformation along with a three-dimensional fault geometry.
5. **Understanding the role of subducting ridges and rifts on Himalayan tectonics:** Since the ridges and rifts are often observed to act as a barrier for the rupture extent of large earthquakes, characterizing and quantifying their role in fault geometry and strain accumulation (using GPS observations) will be an essential task to assess the future seismic hazard in a realistic manner.

6. **Seasonal modulation in GPS time-series:** Seasonal variations influence short term crustal deformation, generally caused by non-tectonic processes such as atmospheric changes or tidal effects. Therefore, modulation of seasonal variations will provide a better understanding of the temporal variations in the associated crustal deformation.
7. **Physical interpretation of the nowcasting approach:** The empirical nowcasting analysis is built on the “short-term fault memory” based renewable or seismic cycle model, in which it is assumed that all accumulated strain will release in a single event. This means that there would not be any “leftover” stress amount, unlike the developing concept of “earthquake supercycles” in great earthquake that exhibit “long-term fault memory” [250].
8. **Improved seismic hazard map and scenario (hypothetical) earthquake studies:** Considering various factors, such as the pattern of short term crustal deformations, strain distributions, long term slip estimations, and recurrence interval of large magnitude earthquakes, the existing seismic hazard map of the study region may be revised. In addition, the present findings may be useful to develop scenario or hypothetical earthquake models for a prior understanding of the probable earthquake damages in a seismically active region.
9. **Seismic risk mapping:** As the present thesis has provided valuable inputs for the seismic hazard analysis along the Himalayan arc, the seismic risk mapping based on the consideration of vulnerability and other aspects may be carried out as a future work.